Bulletin of the Earthquake
Research Institute
Vol. 43 (1965), pp. 241-267

18. *Gravimetric and Geomagnetic Studies of Onikobe Area.*

By Tsuneji Rikitake, Hirokazu Tajima, Sadakatu Izutuya, Yukio Hagiwara, Kaoru Kawada and Yoichi Sasai,

Earthquake Research Institute.

(Read March 23, 1965.—Received March 31, 1965.)

Summary

Gravity and magnetic surveys over the Onikobe area, which, occupying the north-west corner of the Miyagi Prefecture, is famous for a caldera-like topography, are described. It is the aim of these surveys to supplement an aeromagnetic survey conducted by Y. Kato and others as one of the targets of the project named "Combined Aeromagnetic-Gravity Studies of Calderas in Japan", U.S.-Japan Cooperative Science Program.

A marked gravity low associated with magnetic highs was discovered in the central portion of the area. A depression of granitic basement of 1800 m in depth is presumed there. The magnetic highs seem to be associated with andesite lavas forming the peaks which look like central cones. This data strongly suggests that the Onikobe area is a sort of caldera, this conclusion seeming to harmonize with the present geological view.

1. Introduction

The Onikobe area at the north-west corner of Miyagi Prefecture (Fig. 3) is famous for its caldera-like topography. Surrounded by a range of somma-like mountain peaks such as Yadateyama, Oshibayama, Koshibayama, Kamurodake, Katakurayama and so on, a roughly circular area of about 30 km^2 looks like a caldera floor in which are found geisers, hot springs and geothermal areas. The central portion of the area is occupied by a few peaks, Araodake, Hachimori and so on, so that these peaks look like central cones of a typical caldera structure. It is also interesting to note that a river starting somewhere at the eastern foot of these peaks encircles the margin of this area. Simplified topography of the Onikobe area is reproduced in Fig. 1.

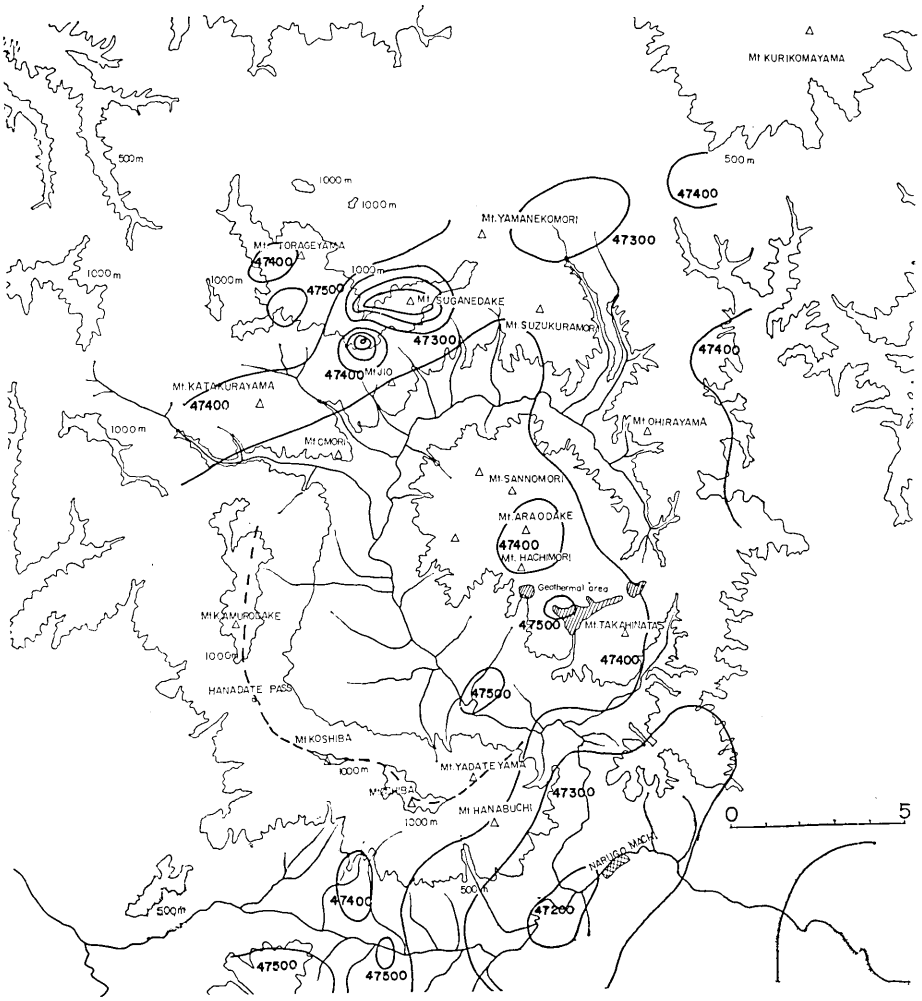

Fig. 1. Simplified topography of the Onikobe area. Full lines are contour lines for the total magnetic intensity in units of gamma at a height of 5000 ft above sea level. Broken line indicates the so-called caldera rim. Geothermal areas are shown by hatched areas.

Since 1963, a project[1] called "Combined Aeromagnetic-Gravity Studies of Calderas in Japan" has been under way as one of the projects of the U. S.-Japan Cooperative Program. Calderas such as Kutcharo, Toya, Towada, Hakone, Aso, Aira and so on were surveyed either by an American or a Japanese airplane. Professor Y. Kato and

1) Report on the Review Meeting on Combined Aeromagnetic-Gravity Studies of Calderas in Japan published by the Japan Society for the Promotion of Science (1964).

others conducted a magnetic survey over the Onikobe area with a helicopter-borne proton precession magnetometer. A simplified version of the magnetic chart for total geomagnetic intensity is reproduced also in Fig. 1 with Professor Kato's permission.

The Onikobe area was chosen as one of the targets over which a detailed aeromagnetic survey should be conducted because there has been much debate whether or not it is a caldera formed by engulfment. Even the possibility that it is a resurgent cauldron (after Smith and Baily) has been suggested by some geologists. Since no existing data of gravity were available there, a detailed gravity survey was planned by the Earthquake Research Institute with the support of the Japan Society for the Promotion of Science. A land magnetic survey was also undertaken. Actual gravity survey was made by Tajima and Izutuya, while Kawada and Sasai carried out the magnetic survey. Hagiwara worked on the programming for terrain correction and interpretation of data by use of an IBM 7090 computer.

Geology of the Onikobe area will be briefly outlined in Section 2 on the basis of a published geologic map and on what the writers were informed of by geologists. Following Section 2, the results of the gravity survey will be reported in Section 3 together with the Bouguer anomalies over the area. The method used for the terrain correction can be seen in the Appendix at the end of the paper. In Section 4 will be outlined the land magnetic survey and its results. Combining all these results, an attempt to form a possible model of underground structure will be made in Section 5.

2. Geology in brief

A simplified geologic map of the area, based on the 1 : 75000 scale quadrangle map "Onikobe" published by the Geological Survey of Japan[2], is shown in Fig. 2. The authors do not state explicitly that the Onikobe area is a caldera but describe it as a composite structural depression bounded by faults. However, H. Kuno[3] considered this area as an example of the calderas of Krakatau type[4], i. e. volcanic depression formed by a collapse following outpouring of a large amount of

2) N. KATAYAMA and K. UMEZAWA, 1:75000 geological map and explanatory text "Onikobe." Geol. Surv. Japan, (1958).

3) H. KUNO, *Trans. Am. Geophys. Union*, **34** (1953), 267.

4) H. WILLIAMS, *Univ. Calif. Pub., Bull. Dept. Geol. Sci.*, **25** (1941), 239.

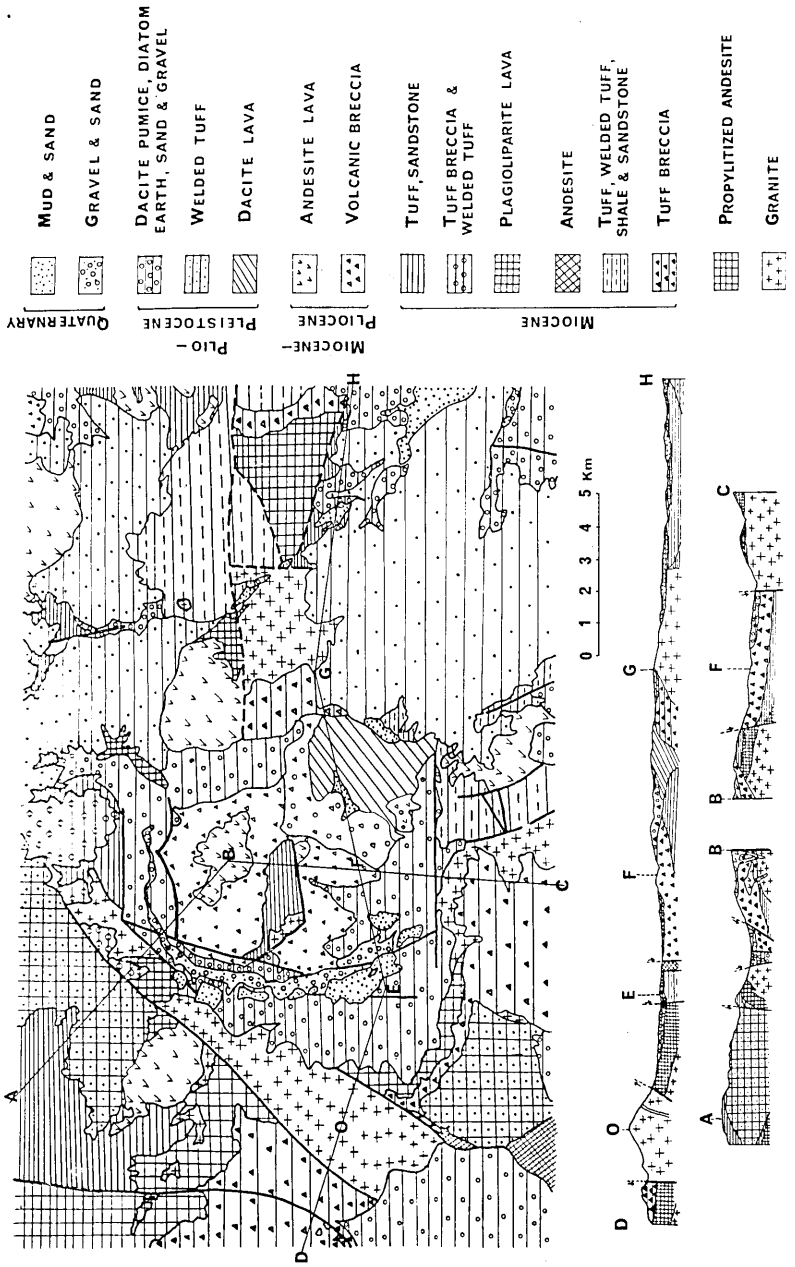

Fig. 2. Simplified geologic map of the Onikobe area.

pyroclastic materials in the form of pyroclastic flow. Y. Katsui[5] described welded tuffs which extend over a wide area mainly east of the Onikobe area (see Fig. 2), and considered that the welded tuff was formed by a large-scale eruption which preceded the formation of the Onikobe caldera.

Recent geologic work by many investigators, still mostly unpublished, indicates that the welded tuff mentioned above is too young (Pleistocene) to be directly related with the subsidence which probably took place during Miocene. On the other hand, a very marked ring structure composed mainly of concentric arrangements of volcanic rock units has been found in the area indicating the presence of structure caused by cauldron subsidence and possible subsequent adjustment.

Therefore, at present, geological data strongly supports the structure closely related to a caldera, with a diameter of about 10 km, which must have been produced by the Neogene volcanic activity. Presence of Miocene volcanic strata similar to those distributed outside the caldera rim and small stocks of granitic rocks within the presumed caldera has led some geologists to suspect that the structure is a resurgent caldera as defined by Smith and Bailey[6].

3. Gravity study

3-1. Gravity survey

A gravity survey by use of a La Coste and Romberg Geodetic gravity meter No. 34 was conducted over the Onikobe area during the periods June 10—19 and Sept. 7—19, 1964. 73 stations distributed over an area approximately 20 km × 40 km were occupied. The distribution of the gravity stations is shown in Fig. 3.

Station No. 1 was chosen as a temporary base station. The gravity value there was directly connected to the one at the fundamental gravity station in Tokyo in the basement of the Chemical Institute, University of Tokyo. It was confirmed that the difference in gravity value between these two stations was kept within a range of 0.005 mgal throughout the survey period. On the way from Tokyo to Onikobe and back, gravity at a first order levelling station B. M. 5400 in Sendai was measured four times. Comparing the results with those measured by the Geographical Survey Institute in 1954, it turned out that the difference in gravity value there between the two series of measurements amounted

5) Y. KATSUI, *Journ. Jap. Assoc. Min. Petr. Econ. Geol.*, **39** (1955), 190.

6) R. L. SMITH and R. A. BAILEY, Abstracts of Intern. Symp. Volcanol. (1962), 67.

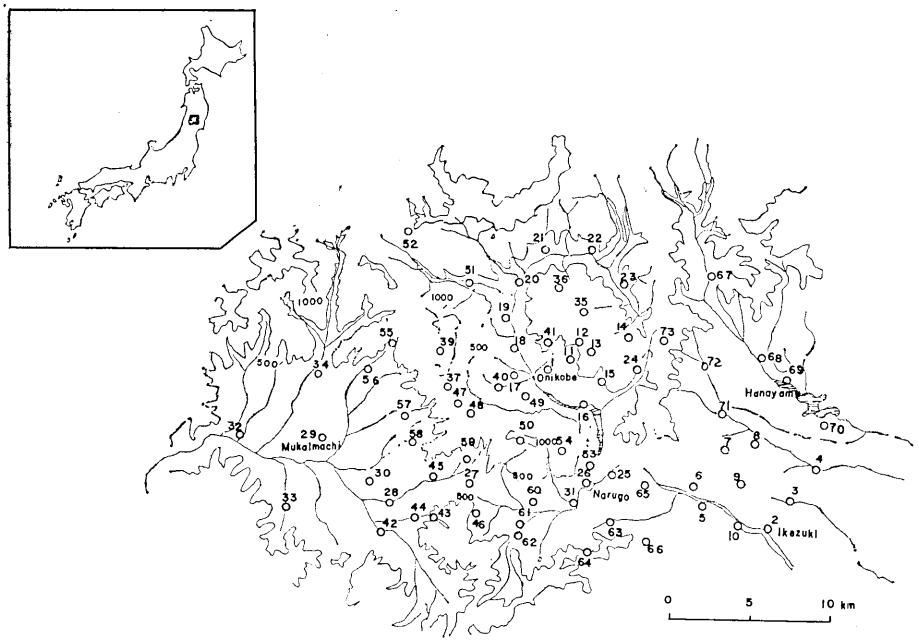

Fig. 3. Locality of the Onikobe area and the distribution of the the gravity stations. The 500 and 1000 m contours are also indicated.

to only 0.07 mgal. In the light of these comparisons, it can safely be said that the gravity value at the temporary base station is accurate enough for the present survey. Gravity values at each field station were then determined relative to the gravity value at the base station.

Since the area concerned is mountainous, it was no easy matter to determine the height of a gravity station. Therefore as many levelling stations, triangulation points and spot heights as possible were occupied in order to rely on the heights already established. Among 73 stations, it was possible to occupy 36 stations where the height was known. For remaining stations, the height was determined from aerophotographs with the help of measurements by an Askania micro-barometer and topographical maps on a scale of 1/1000 which was supplied from the local town office. In practice, a station chosen in the field was marked on the aerophotograph. The height of the mark was later determined by making use of a Zeiss Stereotope. The accuracy of such a determination depends on whether or not we have control points, where the heights are well-determined, on the same map. It is generally believed, however, that the above procedure provides a height determination with

an accuracy of ±3 m even in the worst condition.

The observed gravity values at respective stations are indicated in Table 1 together with the localities, longitudes, latitudes and heights of stations.

3-2. Corrections and anomalies

The observed gravity value g was corrected for free air anomaly in a customary way by adopting 0.3086 mgal/m as usual. Free air correction δg_0 is also shown in Table 1.

The corrected value g_0 thus obtained was subjected to terrain correction of which the detail of programming for an IBM 7090 computer will be seen in the Appendix. A 40 km × 40 km square net of 1 km meshes is placed over maps on a scale of 1/50000 in such a way that the centre of the net coincides with the point where the correction is required. Heights at each grid point are then read off. These values are subsequently used for the terrain correction according to the scheme described in the Appendix. As for the extent of area required for the correction, we know from the previous experience from Mt. Fuji that the correction arising from outside the net amounts to 5 mgal or so even for a station 2500 m in altitude from the sea level. In the present survey the elevation at the highest station does not exceed 1300 m, so that the effect outside the net adopted would not be important.

It is further required for estimating terrain correction as well as Bouguer anomaly to determine the mean density which should effectively be used over the area concerned. As there seems to be no unique way of doing this, a new method was applied to the present case. Gravity value g_h at a point of h in height is given by

$$g_h=\gamma_0-h\partial g/\partial z+2\pi k^2\rho h-\delta t\ , \qquad (1)$$

where γ_0 is the standard gravity, k^2 the gravitational constant, ρ the mean density, δt the terrain correction, and $\partial g/\partial z$ the vertical gradient of the gravity. Hence it is seen that $g_h-\gamma_0+\delta t$ is correlated linearly to h with a proportional constant $\partial g/\partial z-2\pi k^2\rho$.

As ρ is involved in δt, it is not possible to immediately determine ρ from such a relation. An approximate approach is effected as follows. First of all, we ignore δt and plot $g_h-\gamma_0$ against h as can be seen in Fig. 4 in which a linear relation between $g_h-\gamma_0$ and h is well demonstrated. By applying the method of least square, $\partial g/\partial z-2\pi k^2\rho$ is then calculated. If we assume a normal value 0.3086 mgal/m for $\partial g/\partial z$, ρ in units of g/cm^3 is estimated as 1.97. If we assume that ρ_t (the density

Table 1. Locality of the gravity stations and the gravity values.

ϕ: Latitude
λ: Longitude
H: Height above sea level
g: Gravity
δg_0: Free air correction
$\delta g_0'$: Terrain correction
$\delta g_0''$: Bouguer correction
γ_0: Standard gravity
Δg_0: Free air anomaly
$\Delta g_0''$: Bouguer anomaly

No.	Locality	ϕ	λ	H (m)	g (gal)	δg_0 (mgal)	$\delta g_0'$ (mgal)	$\delta g_0''$ (mgal)	γ_0 (gal)	Δg_0 (mgal)	$\Delta g_0''$ (mgal)
		38°N	140°E		960.				980.		
1	Onikobe Lodge 鬼首ロッヂ	48.0	40.2	331	04265	102.2	1.5	−31.5	07433	+70.5	+40.5
2	Ikezuki, S. H. 池月 S. H.	42.6	49.9	87	11592	26.9	0.6	− 8.3	06640	76.4	68.7
3	Path N. of Mt. Myoho, B. M. 名法山北 (2nd B. M. 附近)	43.8	50.2	228	09358	70.4	0.6	−21.7	06816	95.8	74.7
4	Kozo, S. H. 小僧 S. H.	44.6	51.7	114	12087	35.3	1.0	−10.8	06934	86.7	76.9
5	Shiraito falls 白糸滝	43.4	46.9	117	11604	36.1	2.5	−11.1	06758	84.6	75.9
6	Kawatabi, B. M. 川渡 (2nd B. M. 附近)	44.1	46.6	126	11289	38.9	4.3	−12.0	06860	83.2	75.4
7	Uehara, T. P. 上原 T. P.	45.3	47.7	349.3	05278	107.9	0.7	−33.2	07037	90.2	57.6
8	Hill S W. of Otaki, S. H. 大滝南西 S. H.	45.5	49.1	272	06401	83.9	1.5	−25.9	07066	77.3	52.9
9	Hill S. of Uehara, S. H. 上原南 S. H.	44.2	48.5	317	06976	97.9	1.0	−30.2	06875	98.8	69.7
10	Sakaimatsu 堺松	42.9	48.4	101	11553	31.2	1.1	− 9.6	06684	79.9	71.4
11	Path NE. of Fukiage, S. H. 吹上北東 S. H.	48.3	41.1	482	01741	148.8	4.8	−45.9	07477	91.4	50.4
12	Megamaogama fumarole 女釜.男釜	48.9	41.7	456	01862	140.7	13.2	−43.4	07565	83.7	53.5
13	Katayama pass, S. H. 片山峠 S. H.	48.5	42.1	673	979. 98659	207.7	3.6	−64.0	07506	119.2	58.8

14	Hill S. of S.H. of Arayu	荒湯S.H.の南	48.9	43.9	628	99810 980.	193.8	4.7	−59.7	07565	116.3	61.2
15	Diverging point of Kamitaki and Kanisawa	神滝蟹沢分岐点	47.7	42.6	544	01003	167.9	2.6	−51.8	07389	104.0	54.9
16	Kobukazawa, S. H.	小深沢 S. H.	46.9	41.9	271	07282	83.6	2.5	−25.8	07271	83.7	60.4
17	Hill W. of Hara, T. P.	原西方 T. P. 附近	47.8	38.7	345.9	03868	106.7	1.9	−32.9	07403	71.4	40.4
18	Tano, S. H.	田野 S. H.	48.5	38.9	316	04278	97.5	1.9	−30.1	07506	65.2	37.1
19	Ishibuchi shrine	石淵神社	47.9	38.5	345	04704	106.5	2.9	−32.8	07682	76.7	46.8
20	Senbokuzawa	仙北沢	51.0	39.0	316	05626	97.5	12.4	−30.1	07873	75.1	57.4
21	Nuruyu, S. H.	寒湯 S. H.	51.8	40.3	367	05166	113.3	3.7	−34.9	07991	85.0	53.8
22	Horonai	保呂内	51.7	42.1	384	04885	118.5	2.8	−36.5	07976	87.6	53.9
23	Bridge SW. of Mt. Ohira	大平山南西	50.7	43.6	421	04367	129.9	1.9	−40.1	07829	95.3	57.1
24	Diverging point of Rokkaku stock farm	六角牧場入口	47.7	44.1	468	03793	144.4	1.0	−44.5	07389	108.5	64.9
25	Narugo, B. M.	鳴子 2nd B.M. 附近	44.6	43.3	161	09303	49.7	2.3	−15.3	06934	73.4	60.3
26	Narugo tunnel, S. H.	鳴子隧道 S.H.	44.2	41.9	235	07657	72.5	2.6	−22.4	06875	80.3	60.5
27	Sakaida, B. M.	堺田 B. M. 附近	44.0	37.4	354	03798	109.2	5.7	−33.7	06846	78.8	50.8
28	Myojin bridge, B. M.	明神橋際 2nd B. M. 附近	43.5	33.8	243	06408	75.0	1.5	−23.1	06772	71.4	49.7
29	Sawahara, S. H.	沢原 S. H.	45.6	31.0	207	06024	63.9	1.1	−19.7	07081	53.3	34.7
30	Tomisawa, S. H.	富沢 S. H.	44.1	33.0	227	05763	70.1	1.1	−21.6	06860	59.1	38.6
31	Narugo canyon, B. M.	鳴子峡 2nd B. M.	43.6	41.5	272.2	06530	84.0	1.1	−25.9	06787	81.4	56.6
32	Usugi, S. H.	鵜杉 S. H.	45.7	27.6	173	08586	53.4	1.9	−16.5	07095	68.3	53.8
33	Irinosugi, S. H.	入の杉 S. H.	43.4	29.6	240	06999	74.1	1.6	−22.8	06758	76.5	55.3
34	Nakami, S. H.	仲神 S. H.	47.8	30.9	266	07428	82.1	1.9	−25.3	07403	82.3	58.9

(to be continued)

(continued)

No.	Locality		ϕ	λ	H (m)	g (gal)	δg_0 (mgal)	$\delta g_0'$ (mgal)	$\delta g_0''$ (mgal)	γ_0 (gal)	Δg_0 (mgal)	$\Delta g_0''$ (mgal)
35	Mt. Araodake, T. P.	荒雄岳 T. P.	49.8	41.7	984.2	979. 90628	303.7	8.5	−93.6	07697	133.0	47.9
36	Mountain NW. of Sannomori, T. P.	山王森北西 T. P.	50.7	40.8	938.4	91486	289.6	10.8	−89.3	07829	126.2	47.7
37	Hanadate pass, S. H.	花立峠 S. H.	47.3	36.3	801	96403	247.2	8.2	−76.2	07330	137.9	70.0
38	Fudo-son small shrine of Mt. Kamurodake	禿岳不動尊	48.5	35.9		85308						
39	Mt. Kamurodake, T. P.	禿岳 T. P.	48.5	35.9	1261.7	84913	389.4	21.7	−120.0	07506	163.4	65.1
40	Daishimizu dam	大清水ダム	47.7	38.2	312	980. 04750	96.3	4.6	−29.7	07389	69.9	44.8
41	Mountain N. of Onikobe Lodge, T. P.	鬼首ロッヂ北 T. P.	48.7	40.2	578.7	979. 98839	178.6	4.8	−55.1	07535	91.6	41.3
42	Akakura bridge	赤倉橋際	42.6	33.4	266	980. 06282	82.1	1.1	−25.3	06640	78.5	54.3
43	Upper stream of Suezawa	末沢上流	43.0	36.0	388	02377	119.7	9.6	−36.9	06699	76.5	49.2
44	Suezawa S. of Sasamori	笹森南・末沢	43.0	34.9	354	02929	109.2	1.4	−33.7	06699	71.5	39.3
45	Bridge S. of Mt. Nukazuka	糠塚山南	44.3	35.6	277	05265	85.5	1.7	−26.4	06890	69.2	44.6
46	Valley SW. of Jingamori	陣ケ森南西	43.3	37.6	328	04060	101.2	2.2	−31.2	06743	74.4	45.4
47	Mountain between Hanadate pass and Mt. Koshiba	花立峠・小柴山中間	46.8	36.9	990	979. 91482	305.5	13.1	−94.2	07257	147.8	66.7
48	Mt. Koshiba, T. P.	小柴山 T. P.	46.3	37.7	1055.8	89451	325.8	16.4	−100.4	07183	148.5	64.5
49	Komukai	小向	47.3	39.5	336	980. 04533	103.7	13.5	−32.0	07330	75.7	57.2
50	Mt. Oshiba, T. P.	大柴山 T. P.	45.6	39.3	1082.3	979. 89179	334.0	13.2	−103.0	07081	155.0	65.3
51	Fudo falls	不動滝	50.9	37.0	369	980. 05029	113.9	12.4	−35.1	07858	85.6	62.9
52	Onikobe pass, T. P.	鬼首峠 T. P.	52.6	34.6	868.9	979. 94929	268.1	2.5	−82.7	08108	136.4	56.2
53	Narugo dam	鳴子ダム	45.1	42.5	259.5	980. 07367	80.1	8.8	−24.7	07007	83.7	67.8

54	Mt. Hanabuchi, T. P.	花淵 T. P.	45.3	41.0	984.8	979. 91081	303.9	14.0	−93.7	07037	144.4	64.7
55	Shinnosawa dam	清水沢堰堤	48.8	33.9	405	980. 04580	125.0	9.0	−38.5	07550	95.3	65.7
56	Shinnosawa	清水沢	48.0	32.9	334	05903	103.1	2.1	−31.8	07433	87.8	58.1
57	Path NE. of Hanya	判屋北東	46.5	34.3	348	03974	107.4	1.7	−33.1	07213	75.0	43.6
58	Hotokezawa	仏沢	45.4	34.5	309	04623	95.4	1.8	−29.4	07051	71.1	43.5
59	Path NE. of Matsune	松根北東	45.0	37.2	421	03645	129.9	2.3	−40.1	06993	96.4	58.7
60	Nakayama	中山	43.5	39.8	280	05956	86.4	1.3	−26.6	06772	78.3	52.9
61	Minamihara	南原	43.0	39.4	287	05137	88.6	1.3	−27.3	980. 06699	73.0	46.9
62	Junction of Iwado and Kumazawa valley, S. H.	岩堂熊沢合流点 S. H.	42.5	39.3	255	06113	78.7	2.3	−24.3	06626	73.6	51.6
63	Numai	沼井	42.9	43.1	266	07654	82.1	5.5	−25.3	06684	91.8	72.0
64	Path between Numai and Mt. Kunimi	沼井.国見山中間	42.0	41.9	465	03318	143.5	1.4	−44.2	06552	111.2	68.3
65	Tanaka, B. M.	田中 2nd B.M. 附近	44.4	44.4	132.4	09712	40.9	2.6	−12.6	06904	68.9	58.9
66	Kayohara	通原	42.1	44.8	225	08865	69.4	2.6	−21.4	06567	92.4	73.7
67	Izune bridge, S. H.	伊豆根橋 S. H.	51.2	47.2	271	08683	83.6	4.2	−25.8	07902	91.4	69.9
68	Omukai	大向南	48.7	49.0	172	10241	53.1	1.9	−16.4	07535	80.1	65.6
69	Mido	御堂	47.7	50.4	127	11235	39.2	1.1	−12.1	07389	77.7	66.7
70	Aidosaka	合道坂	46.3	51.9	126	11593	38.9	0.5	−12.0	07183	83.0	71.5
71	Ozasa dam	大笹堰堤	46.5	47.8	237	07455	73.1	1.8	−22.6	07213	75.6	54.8
72	Karuizawa	軽井沢	48.5	46.8	332	06158	102.5	1.5	−31.6	07506	89.0	58.9
73	Kunimi pass	国見峠	49.1	45.5	529	02533	163.3	2.4	−50.3	07594	112.6	64.7

Remark: T. P. means triangulation point, B. M. bench mark of 2nd class levels and S. H. spot height.

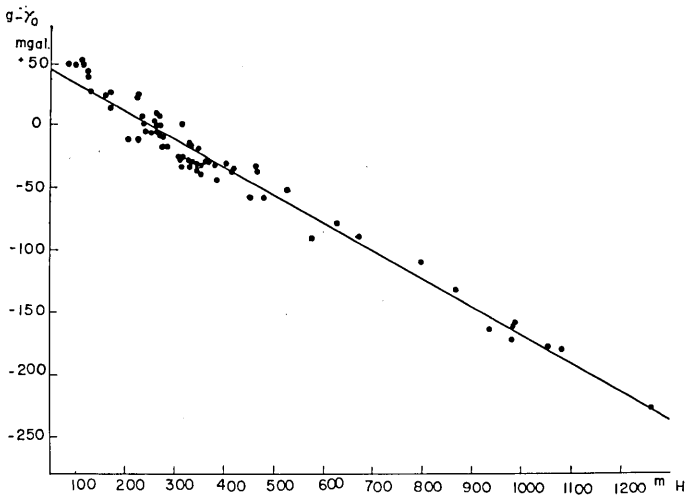

Fig. 4. g_h-γ_0 (gravity anomaly) versus h (height of station) relationship. No terrain correction.

effective for terrain correction) is 2.05, a similar calculation leads to 2.24. If $\rho_t=2.25$, we get $\rho=2.27$. Such changes in ρ by various selections of ρ_t are shown in Table 2. It is thus suggested that $\rho_t=2.28$, which results in $\rho=2.27$, would be adequate for the mean density. The relation between $g_h-\gamma_0+\delta g_0'$ and h is shown in Fig. 5, $\delta g_0'$ denoting the terrain correction finally estimated.

Table 2. Changes in the mean density (ρ) with those in the density for computing terrain correction (ρ_t).

ρ (Density used for computing terrain correction)	ρ (Mean density calculated by the method of least squares)
	1.97
2.05	2.24
2.25	2.266
2.28	2.268
2.40	2.285
2.67	2.32

Once ρ is estimated, Bouguer corrections $\delta g_0''$ at respective stations are easily calculated. In Table 1 are also shown g_0', $\delta g_0''$, γ_0 by the international formula, free air anomaly Δg_0 and Bouguer anomaly $\Delta g_0''$.

3—3 Distribution of Bouguer anomaly

The distribution of Bouguer anomaly is shown in Fig. 6. It is

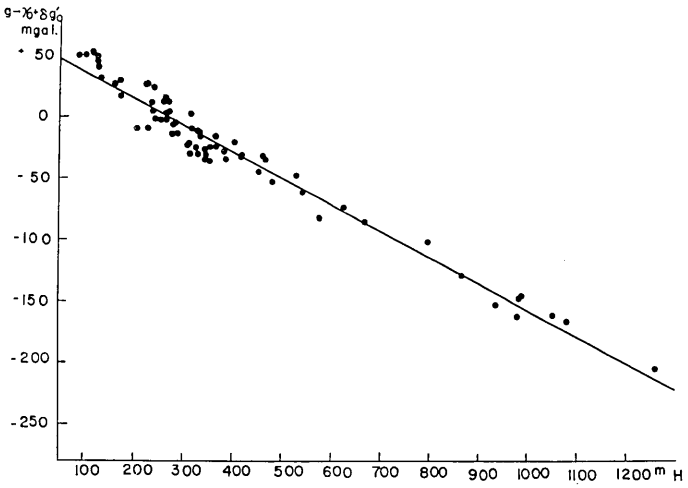

Fig. 5. $g_h-\gamma_0+\delta g_0'$ (gravity anomaly after terrain correction) versus h relationship.

clearly observed that there exists a negative anomaly amounting to 30 mgal in the area which has been suspected of being a caldera. Along the somma-like mountain range, we observe a belt of positive anomaly though nothing is known towards the north of the negative anomaly. It is also noticeable that other negatives are found towards the south-western and south-eastern parts of the area surveyed.

4. Geomagnetic study

The aeromagnetic survey as carried out by Kato and others (Fig. 1) has indicated that relatively small anomalies in the geomagnetic field, say a few hundred gammas at a level of 1700 m in altitude, are associated with the Onikobe area. It seems difficult to make a positive statement about the underground structure there from this survey although some evidence of a magnetization of the so-called central cones was put forward. In the hope of bringing out the geomagnetic anomaly more clearly, a vertical intensity (Z) survey by a Sokkisha GIT magnetometer was undertaken by the Erthquake Research Institute over the Onikobe area during the periods Sept. 8—18 and Oct. 20—27, 1964.

The magnetometer is a sort of flux-gate. When an alternating current (1000 c/s) is applied to a primary coil wound around a permalloy core, a current with a distorted form is induced in the secondary coil

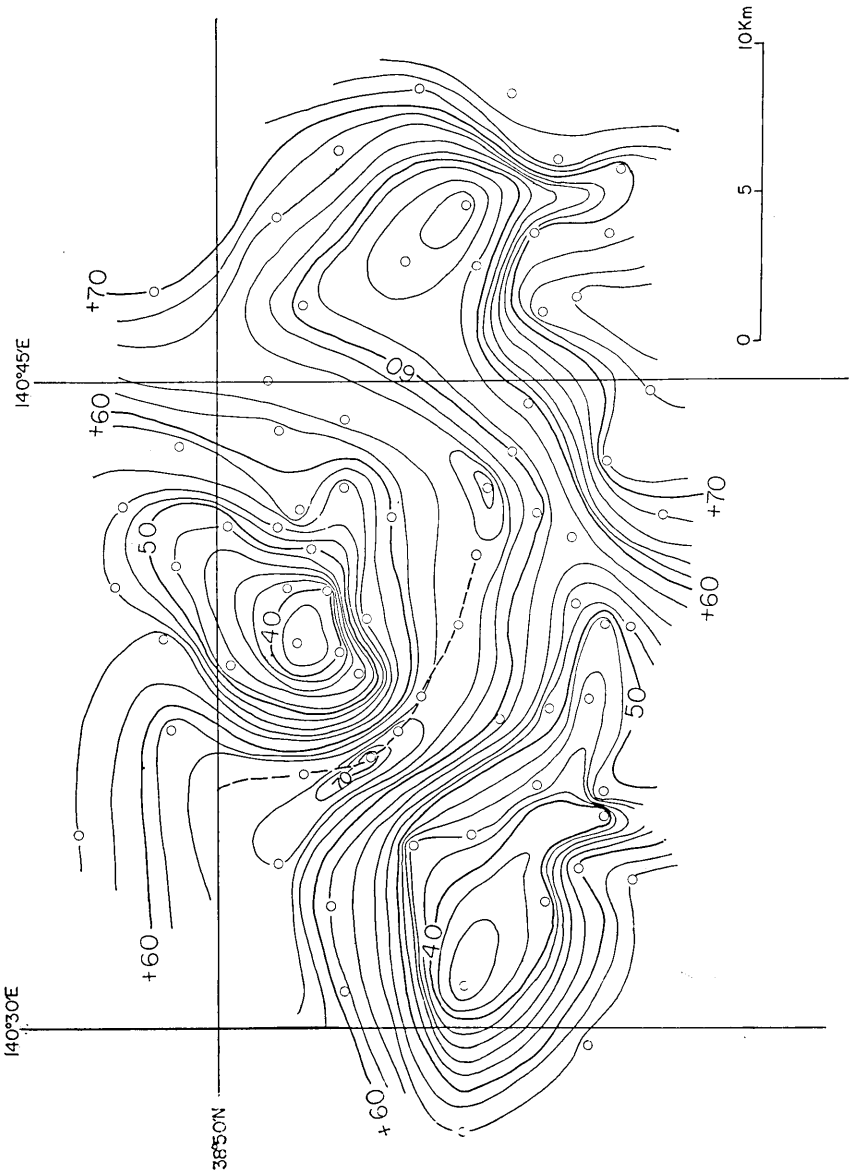

Fig. 6. Distribution of Bouguer anomaly in units of mgal.

because of a non-linear B-H relation of the core. Among the harmonics, the second one is picked up, amplified and finally subjected to a phase-sensitive detection. A direct current controlled by a set of resistances is led to another coil wound on the detector head. If the output is kept at zero by adjusting the direct current so as to cancel the geomagnetic field, the reading of the resistance gives the geomagnetic field intensity to be measured. In a favourable condition, it is said that the accuracy of a measurement is about $\pm 10\gamma$ or so. But in the case of a survey in which a wide variety of temperature cannot be avoided, drift of datum line, slight change in the sensibility and the like have been experienced.

The drift was eliminated by means of measurements at the base station (the same as that for the gravity survey) in the morning and evening of every day. Although it is difficult to estimate the accuracy of each measurement, it is believed that the errors would not exceed a few tens of gammas.

No corrections for daily variation, magnetic storm and such-like were made. Judging from the magnetic records obtained at a magnetic observatory near the area, no large errors could be introduced by such geomagnetic variations because the geomagnetic field was extremely calm during the periods concerned.

Stations amounting to 99 in number were occupied. Although it was hard to establish stations distributed uniformly because of bush and shrubbery, it seems likely that the geomagnetic anomaly over the Onikobe area can be brought to light fairly clearly by the survey. The anomaly in Z is shown in Fig. 7 together with the distribution of stations. The datum of the anomaly values is taken as that at the base station and so the values indicated on the anomaly map are relative.

One of the most outstanding features of the anomaly pattern is certainly the magnetic highs found on the so-called central cones, i. e. Araodake and Hachimori. This suggests that the rocks composing these mountain bodies are strongly magnetized. Although no outcrops were found, there is good reason to think that these peaks are formed by lavas. Hence a typical caldera feature, i. e. gravity lows and magnetic highs, can be seen in the central portion of the Onikobe area.

Over the flat portion of the basin, no marked anomalies are found though a number of magnetic highs are scattered there. A pair of positive and negative anomalies of the order of a few hundred gammas are found around the geothermal area. Whether or not these anomalies

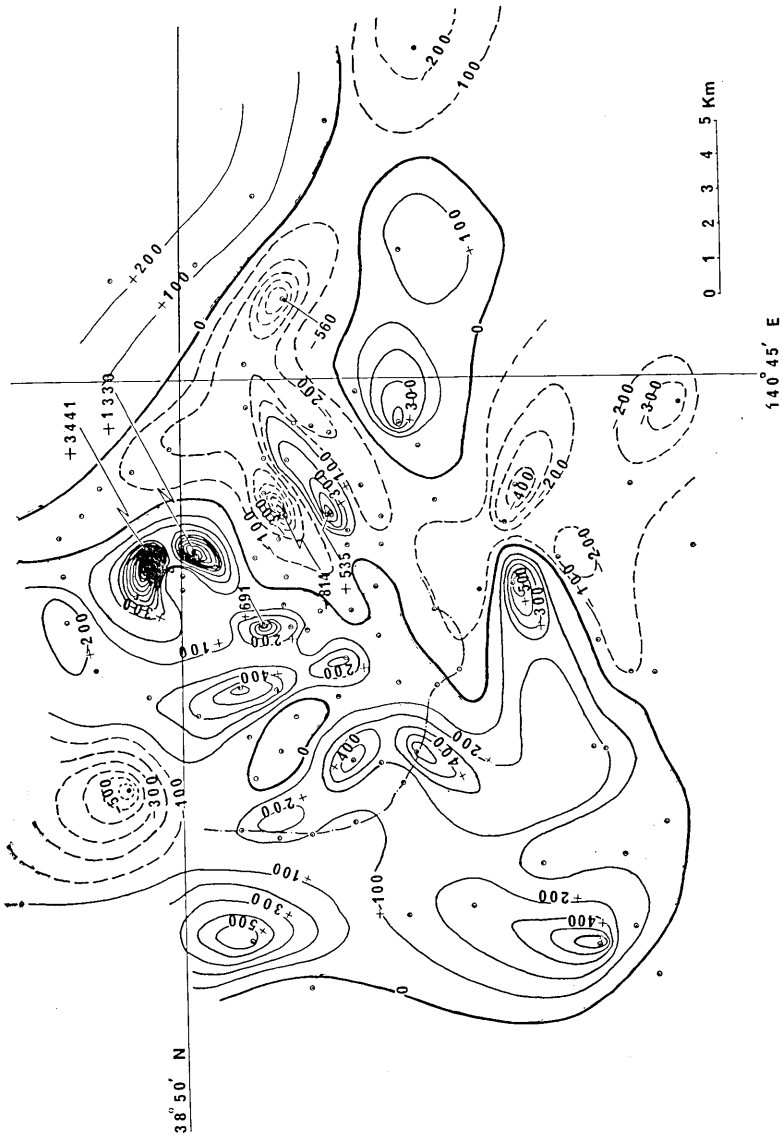

Fig. 7. Distribution of anomaly in the vertical magnetic intensity in units of gamma.

have something to do with the geothermal activity is not known. A number of weak magnetic highs seem to be associated with peaks along the somma-like range. As these anomalies amount to only a few hundred gammas, the magnetizations of rocks composing these mountain bodies would not be strong. One can see, however, that a roughly circular trend of anomaly pattern centred approximately at the centre of the caldera-like topography is prevailing.

It is seen that the anomaly pattern changes suddenly towards the east of the area, one might suspect that such a change is caused by a fault. Although a gravity low of fairly wide extent is found towards the south-west of the area, the magnetic anomaly chart does not indicate a close correlation between gravity and magnetic anomalies. However, the sharp discontinuity of the anomaly pattern from positive to negative towards the south of the area makes us suspect that such a contrast is caused by a fault.

5. Possible model of the underground structure

5—1 Analysis of the gravity data

In order to get at the subterranean structure beneath the Onikobe area from the gravity distribution observed, Kanamori's method[7] for analyzing gravity data was used. The method is essentially a two-dimensional extension of the well-known $\sin x/x$ method[8] for a one-dimensional analysis. Assuming a pre-Miocene granitic basement and overlying coarse layers such as tuff, younger Diluvium and Alluvium beneath the area concerned, a reasonable density contrast between them was chosen at a value between 0.4 and 0.6 g/cm^3, while a range of the depth of datum-plane from 250 to 1,000 m was assumed. The most satisfactory model was achieved by choosing a density contrast of 0.6 g/cm^3 and a datum depth of 500 m. In the actual computation by an IBM 7090 computer, a function subprogramme for Kanamori's formula was compiled.

A basement model computed in such a way is sometimes so crude that the model does not always satisfy the condition that the undulations of the basement should be smaller than the datum depth. For the purpose of arriving at a better model, the gravity distribution due to the first approximation was calculated. Comparing the computed

7) H. KANAMORI, *Proc. Japan Acad.*, **39** (1963), 469.

8) *e. g.* Y. TOMODA and K. AKI, *Proc. Japan Acad.*, **31** (1955), 443.

distribution with the observed one, the depth was modified until the former agreed with the latter. In practice, such a procedure was repeated only twice for obtaining adequate agreement. Fig. 8 shows

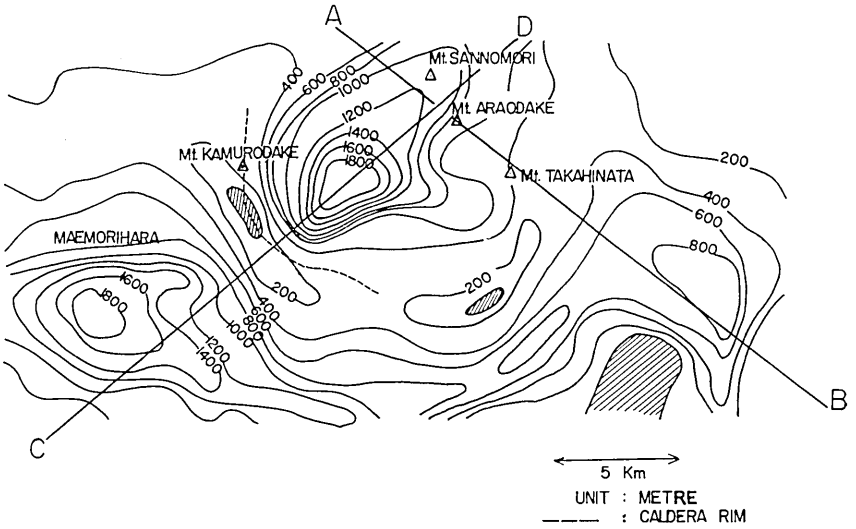

Fig. 8. Estimated depth of basement. Hatched areas indicate outcrops.

the distribution of the basement depth obtained by such a method. The computer programme is analogous to that of terrain correction as will be mentioned in the Appendix. The basement is divided into a number of vertical prisms whose horizontal sections are square. A function subprogramme in which gravity attraction is integrated for all the volume of a prism is prepared for computations of total gravity effect.

The basement depth thus computed for the Onikobe area indicates a roughly circular depression of which the maximum depth amounts to 1900 m. Judging from the underground structure thus brought to light, it seems probable that the depression forms a caldera of Krakatau type. It is doubtful, however, that the depression is a resurgent cauldron as defined by Smith and Bailey[6]. In the case of a resurgent-type structure it is supposed that a dome-up of silicic rocks takes place after the caldera formation, so that we do not observe a gravity low in the central portion of the caldera. It should be emphasized that a marked gravity low is found in the central Onikobe area and that no uplift of basement or intrusion of a pluton of significant size are suggested from the analysis of gravity. Although we observe intense magnetic highs at Mt. Sannomori and Mt. Araodake, it is hardly likely that they are

associated with uplifted domes. It would be more natural to think that these cones were formed by the post-caldera volcanic activities. The mass that forms these cones would be so small that the gravity field is hardly affected.

The caldera is probably of a double structure, because a terrace-like floor extends to the eastern wall of the caldera at a depth of several hundred metres. The fact that geothermal areas are developed over the terrace might suggest that the heat source is shallower in this area than elsewhere in the caldera. The young somma seems likely to coincide with the old one on the southern and western walls.

Gravity highs are distributed circularly along the caldera rim, where the depth of the basement is estimated as 200 m on an average. It is striking that close agreement is found between the computed basement of nearly zero meter depth and the outcrops of granite near Mt. Kamuro.

From the analysis of the negative anomaly situated at the Maemori-hara basin, it is presumed that the anomaly is probably caused by a sinking of the basement to a depth 1,800 m or more. The sinking seems to be a graben rather than a caldera. If it is a caldera, it must have been eroded to a great extent after its formation.

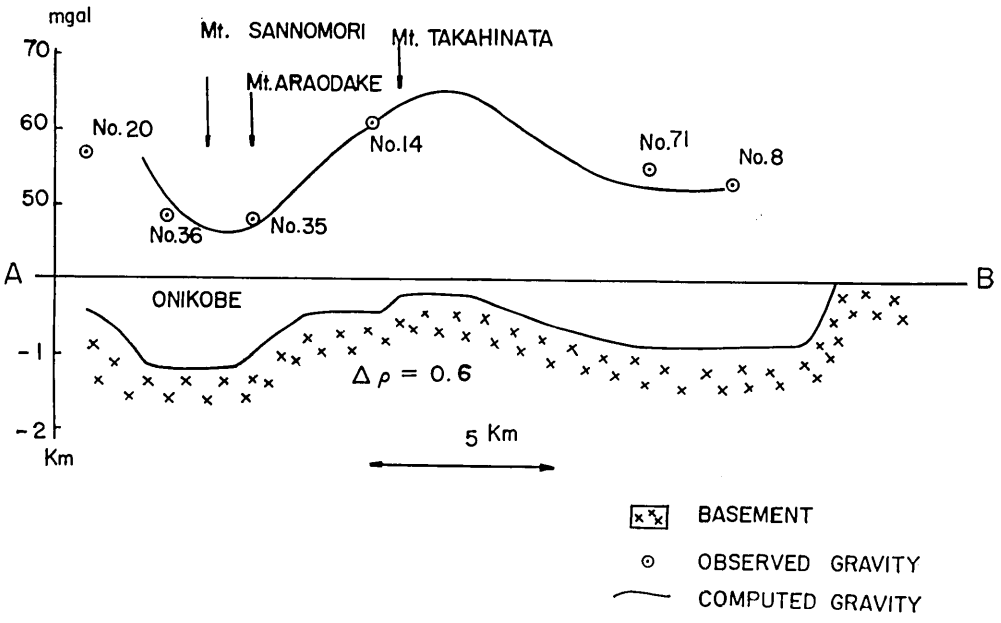

Fig. 9. Estimated profile along the section AB.

Another negative anomaly is found on the eastern flank of the surveyed area. The sinking of the basement, that is likely to be the cause of such a gravity low, seems to have little correlation with the geology and topography at the earth's surface. The maximum depth to the basement surface is estimated as 800 m.

Figs. 9 and 10 show the sections along the straight lines AB and CD indicated in Fig. 8. It is concluded that fairly good agreement can be seen between the gravity values calculated on the basis of the model and those actually measured.

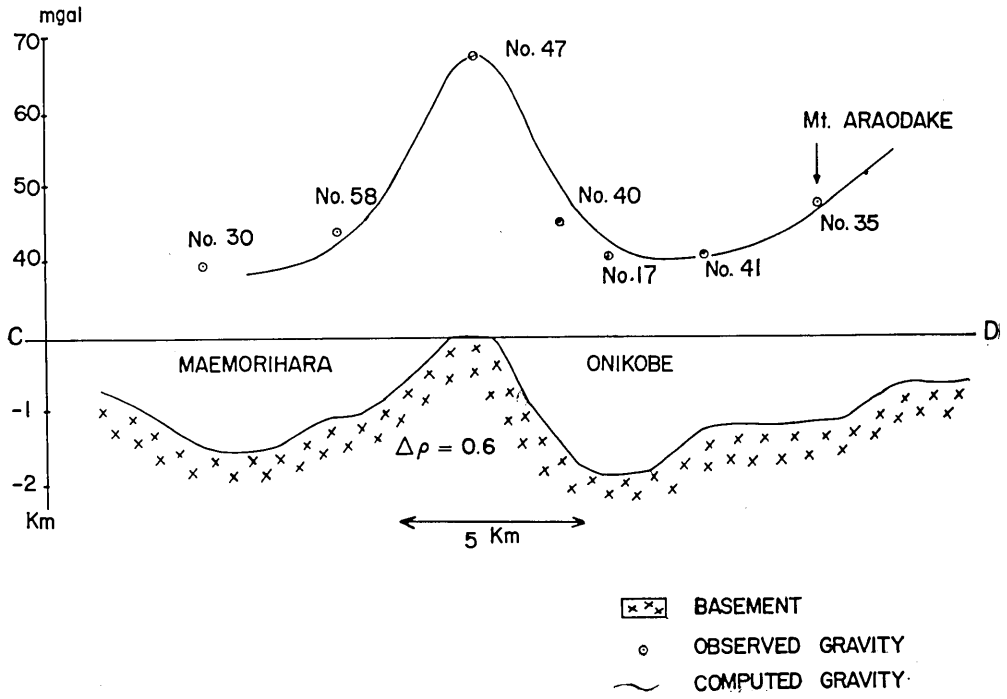

Fig. 10. Estimated profile along the section CD.

5—2 Analysis of magnetic anomaly

The magnetic anomaly over the Onikobe area may approximately be divided into two categories, the one caused by the magnetization of basement blocks and the other by that of andesitic lava flows. The former anomaly, that must have long wavelengths, can easily be separated by a method of two-dimensional frequency analysis from the latter anomaly of short wavelength which is essentially expressed with the fields due to dipoles scattered over the area. The output of the

observed anomaly distribution through a low-pass filter is mapped in Fig. 11. It is seen in the figure that the arrangement of magnetic highs and lows generally agrees with the result of the aeromagnetic survey (Fig. 1). The anomaly of short wavelength is easily obtained by subtracting the anomaly of long wavelength from the original anomaly as has been shown in Fig. 7.

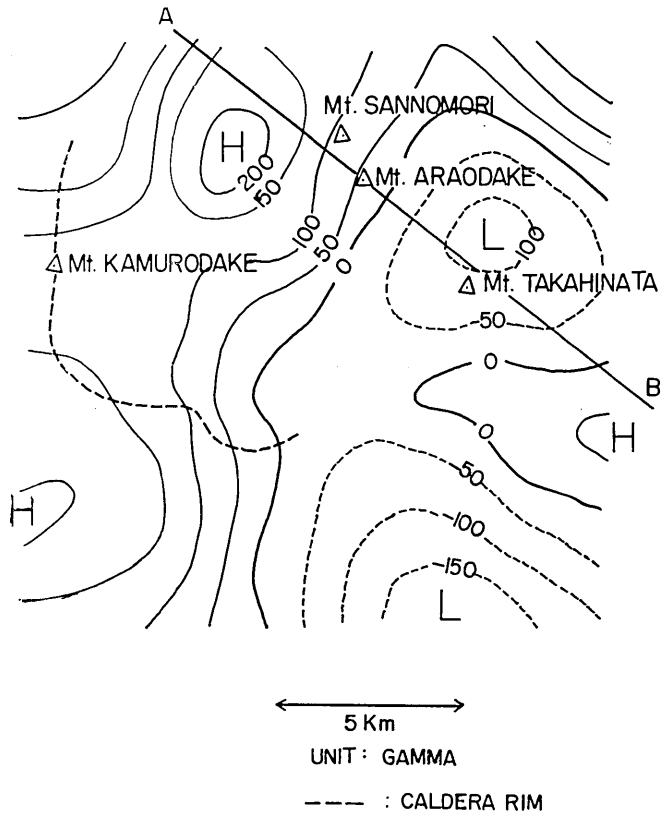

Fig. 11. Magnetic anomaly of long wavelength calculated through a low-pass filter.

5—3 Combined gravity-magnetic interpretation

The anomaly of long wavelength is so broad that no explanation by a near-surface magnetized body is possible. It would be reasonable to assume therefore that the magnetic anomaly of long wavelength could be caused by the magnetization of the same body by which the gravity anomaly is caused.

In the light of the above discussion, a model as shown in Fig. 12 is

supposed for a magnetic profile along AB. A deep magnetic body is assumed beneath the north-western rim of the caldera. It is also assumed that the body extends infinitely westwards. Three magnetic bodies with a fairly intense magnetization are then added in order to account for the magnetic highs observed.

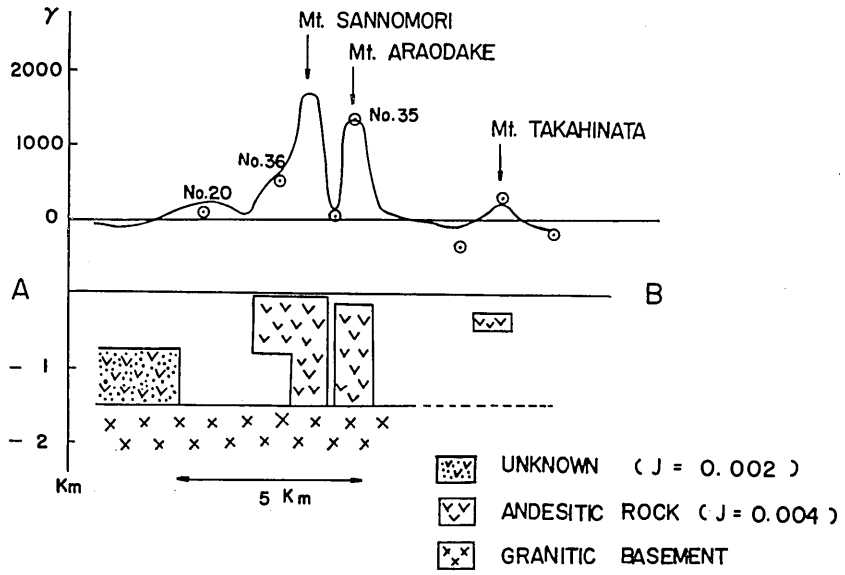

Fig. 12. Magnetic profile along AB.

Assuming that these magnetic bodies are magnetized in the direction of the present geomagnetic field, the magnetic anomalies due to these bodies were calculated for various combinations of their sizes, shapes and intensities of magnetization. Fig. 12 shows a model which gives rise to an anomaly agreeing fairly well with the observed one. The depth and thickness of the magnetic body beneath the north-western rim of the caldera are both estimated as 750 m, while the intensity of magnetization as 0.002 e. m. u./cm^3. It is striking that the depth thus estimated roughly agrees with that deduced from the gravity analysis. As the intensity of magnetization seems too high for an ordinary granite, it is required to assume a body of high magnetization and high density. Whether or not the body is composed of andesitic rocks is not known.

The outstanding magnetic highs around Mts. Sannomori, Araodake and Takahinata can be accounted for if magnetic bodies having shapes as shown in Fig. 12 and an intensity of magnetization amounting to 0.004 e. m. u./cm^3 are assumed. Judging from the intensity of magne-

tization, it would safely be presumed that these anomalies are caused by andesitic rocks. The volumes of these bodies are so small that they hardly affect the gravity distribution.

6. Concluding remarks

Combined gravity-magnetic study of the Onikobe area leads us to a conclusion that the area is closely related to a caldera. But no evidence for a resurgent caldera is found. The maximum depth of the granitic basement is estimated as 1800 m. The magnetic highs associated with the central peaks are believed to be caused by the magnetization of andesitic lava probably welled out during the post-caldera volcanic activity. It is striking that a typical caldera structure, magnetic highs in the middle of a gravity low, can be seen there. It is also interesting that two gravity lows are found towards the south-west and south-east of the Onikobe area although no marked magnetic anomalies are found there.

As the magnetization of rocks composing the Onikobe area and its surroundings are generally weak, the magnetic anomalies as revealed by the aeromagnetic survey are not very strong. It should be pointed out, however, that the long wavelength anomalies obtained from the analysis of the land magnetic survey harmonizes with the aeromagnetic ones.

In conclusion, the writers wish to express their thanks to Professor Kato by whose permission his aeromagnetic results were made available. Much of the geological information was given by Dr. S. Aramaki. The writers are very grateful to him. Acknowldgment is made of the partial financial support for this investigation through a grant from the Japan Society for the Promotion of Science as part of the Japan-U. S. Cooperative Science Program.

APPENDIX: Note on the Terrain Correction

Terrain correction for gravity by use of a high-speed computer has recently become popular. The outline of a terrain correction program on an IBM 7090 computer as developed by one of the authors (Y. H.) and used in this paper will be described in the following.

Bott[9] and Kane[10] independently developed practicable methods for

9) W. P. H. BOTT, *Geophys. Prospect.*, **7** (1959), 45.
10) M. F. KANE, *Geophysics*, **27** (1962), 455.

computation of terrain correction. It has been customary for the correction by a desk machine to divide the area around a gravity station into a number of small segments of annular belts of which the elevations are estimated and then to estimate all the effects due to these segments on the gravity at the station concerned. In the case of terrain correction by use of a digital computer, however, it is more convenient to cover the area with a square mesh, elevations at each grid point being then read on a topographical map of the surveyed area and recorded together with their locations on punched cards. Kane named such a set of digitized data the "digital terrain

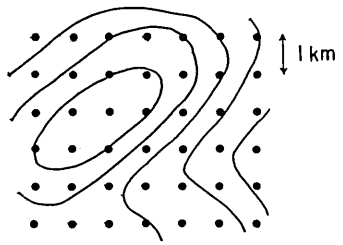

Fig. 13. Topography and square grids.

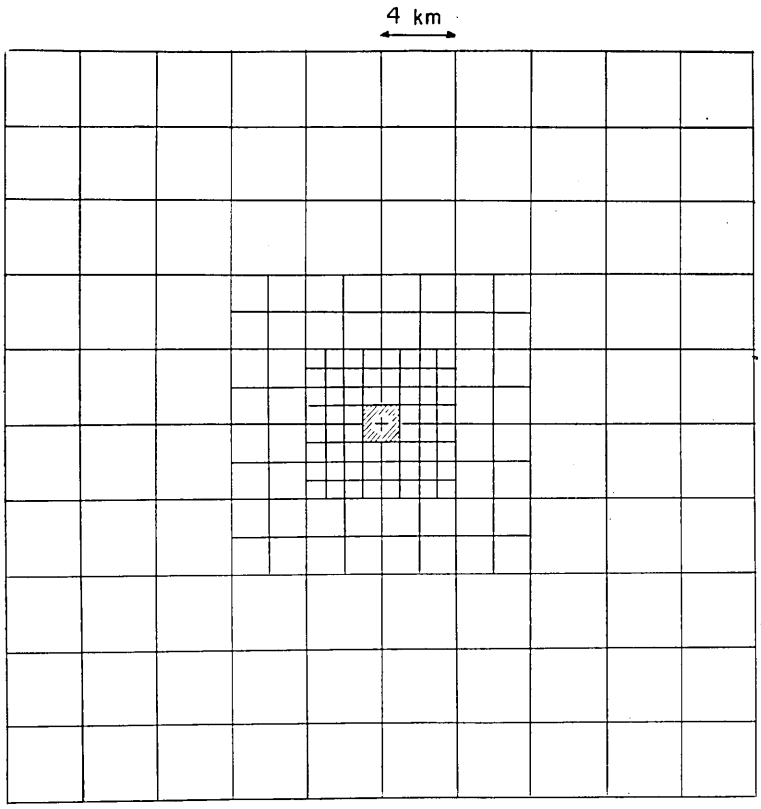

Fig. 14. Net used for terrain correction. The central hatched area is excluded from the correction for the outer area.

model''. 1-km spacing is usually taken for forming a model as can be seen in an example in Fig. 13. Terrain correction for a gravity station is computed by summing-up the gravitational effect of all the prisms with square bases. The square segments are arranged around the station in a fashion as shown in Fig. 14. The central 2 km × 2 km square is excluded from the 1-km spacing scheme because the gravitational effect within that area cannot be computed precisely with 1-km spacing. As a gravity station does not always coincide with one of the grid points of the terrain model, effective elevations are approximately estimated by the following method. As can be seen in Fig. 15, let $H(I, J)$, $H(I+1, J)$, $H(I, J+1)$ and $H(I+1, J+1)$ be the elevations at the grid points. In that case $H(X, Y)$, the effective elevation assumed at the centre of the smallest pattern square, is given by

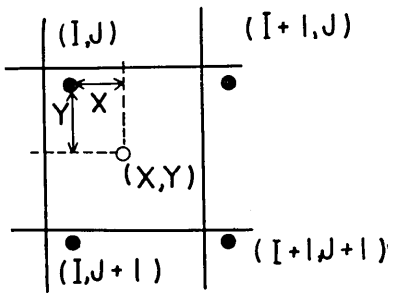

Fig. 15. Position of the smallest pattern and grids on terrain model.

$$H(X, Y)=AXY+BX+CY+D$$

where

$$A=H(I+1, J+1)-H(I, J+1)-H(I+1, J)+H(I, J)$$
$$B=H(I+1, J)-H(I, J)$$
$$C=H(I, J+1)-H(I, J)$$
$$D=H(I, J).$$

In the case of a pattern square of intermediate size the average values of nine elevations $H(X, Y)$'s computed from those at sixteen grid points of the terrain model are adopted, and for the largest pattern square sixteen $H(X, Y)$'s from twenty-five grid points.

Kane approximated the gravity attraction of a prism by that of an annular ring with the same height, while the authors adopted an approximation due to a line-mass concentrated along the vertical axis through the centre of the prism. Although the errors in the case of line-mass approximation are slightly larger than those for Kane's approximation, the errors seldom exceed 1.0 mgal even in mountainous regions. The formula for such an approximation is given as

$$g=k^2\rho A(1/R-1/\sqrt{R^2+H^2}),$$

where g is gravity attraction, k^2 gravitational constant, ρ density, A

area of the horizontal section of the prism, R distance between the centre of the prism and the gravity station, and H height of the prism.

Another program for the terrain correction in the central 2 km × 2 km square is readily formed in a similar fashion. The area is subdivided into twenty-eight square segments (Fig. 16). The gravity attractions due to each segment are then computed and summed-up. In contrast to such a procedure Kane divided the area into eight octants, the surfaces of which are assumed to slope continuously from the apex to the outer edge. Kane's method is convenient for computing the inner area effect because the program for the outer area can include the inner one. But it appears to the authors that the fact that the gravity effect of the inner area sometimes reaches 10 mgal or more necessitates a better approximation.

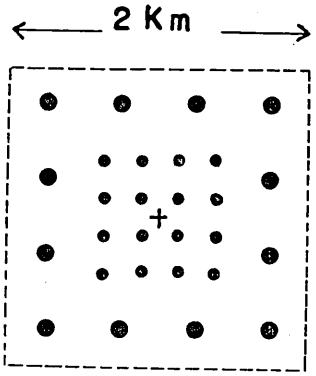

Fig. 16. Division for the inner area correction.

In the Onikobe area terrain corrections were computed for 72 stations. The topography there is so rugged that corrections range from 0.1 mgal to 20 mgal ($\rho=2.27$) or more. The maximum value in the outer area reaches 14.1 mgal, and 8.7 mgal in the inner area. A rectangular mesh 72 km × 61 km was used for the terrain model. The time required for the computing amounted to about 0.9 sec per gravity station for the outer area and about 0.2 sec for the inner.

18. 鬼首地域の重力ならびに磁気測量

地震研究所 { 力武常次 / 田島広一 / 井筒屋貞勝 / 萩原幸男 / 川田薫 / 笹井洋一 }

宮城県鬼首地域はカルデラ状の地形で知られているが，今回同地域においてラコスト重力計ならびに GIT 磁力計による測量を行なつた．日米科学協力の一環として，「日本火山カルデラの航空磁気・重力測量」という協力研究があるが，鬼首地域はその測量対象の一つである．今回の研究は，地上での重力，磁気異常を求め，航空磁気測量の結果とあわせて，同地域の地下構造を明らかにすることを目的とした．

72点に達する重力測定値には，電子計算機 IBM 7090 を使用して，地形補正を施した．このような山間部においては，地形補正は時として 20～30 mgal に達し，本格的地形補正を施さなければ，意味のある解釈に到達することは困難である．このようにして求められた Bouguer 異常は鬼首地域および隣接の2地域に重力が異常に小さい地域があることを明らかにした．

また磁気測量結果からは，鬼首中央部山体が比較的強く帯磁していることを示している．重力が負の地域に点々として高磁力異常があらわれるのは，典型的カルデラ構造である．

地下構造のモデルを仮定して，重力および磁気異常を説明するためには，次のようなモデルがいちばんもつともらしいと思われる．鬼首地域の granitic な基盤は，幅数 km，深さの最大 1800 m に達する凹みを生じていて，その中央部には安山岩質の溶岩が噴出し，中央火口丘の形をしている．このような結果から推定すると，鬼首地域がカルデラであるとする地質学的解釈に反対する理由は全くないと思われる．